12-2007

Experimental Verification of Source Temperature Modulation Via a Thermal Switch in Thermal Energy Harvesting

Robin McCarty
University of Dayton

D. Monaghan
Air Force Research Laboratory

Kevin P. Hallinan
University of Dayton, khallinan1@udayton.edu

Brian Sanders
Air Force Research Laboratory

Experimental Verification of Source Temperature Modulation via a Thermal Switch in Thermoelectric Energy Harvesting

R. McCarty [1]
University of Dayton, Dayton, Ohio, 45469, USA

D. Monaghan[2]
Air Force Research Laboratories, VAS, Wright-Patterson, AFB, OH 45433

K. P. Hallinan [3]
University of Dayton, Dayton, Ohio, 45469, USA

and
B. Sanders [4]
Air Force Research Laboratories, VAS, Wright-Patterson, AFB, OH 45433

This paper provides a description of research seeking to experimentally verify the effectiveness of a thermal switch used in series with TE devices for waste heat recovery for constant and variable source heat input and for variable source thermal capacitance (mass). Using an experimental set-up comprised serially of a fixed heat source, a variable thermal resistance air gap serving as a thermal switch, a thermoelectric device and a heat sink, the time-averaged power output to power input ratios improved up to 15% and 30% respectively for constant and variable heat input in certain design space conditions. The experimental results, as supported by model predictions, suggest that the thermal capacitance of the heat source must be greater than the thermal capacitance of the TE device in order for thermal switching to improve the time-averaged power output to power input ratios of waste heat recovery systems. The results have direct application to aircraft energy harvesting.

Nomenclature

C	Thermal Capacitance (J/kg-K)
Q	Heat dissipation (W)
PR	Output power to input power ratio (%)
P	Output power from TE device (W)
R	Thermal resistance (K-m^2/W)
T	Temperature (^{o}C)
ZT	Thermoelectric device figure of merit
k	Thermal conductivity (W/m-K)
t	Time (sec)
x	Distance (m)

Subscripts

$HIGH$	High resistance setting of thermal potentiometer

[1] Graduate Research Assistant, Mechanical and Aerospace Engineering, 300 College Park.
[2] Deputy Team Lead, Department Name, 2210 Eighth Street.
[3] Chair and Professor, Mechanical and Aerospace Engineering, 300 College Park.
[4] Team Lead, AFRL/VAS, 2210 Eighth Street, AIAA Associate Member.

IN	Input into system
LOW	Low resistance setting of thermal potentiometer
TE	Thermoelectric device
$TE_{,H}$	*H*ot side of thermoelectric device
$TE_{,L}$	*C*old side of thermoelectric device
h	Heat sink heat exchanger
nc	No Control
p	Thermal potentiometer
s	Heat source
sink	Heat sink

I. Introduction

Recently breakthrough developments in thermoelectric devices have been reported showing increases in the ZT value for thermoelectric (TE) device materials from 1 up to 5 [1-3]. Bell illustrated that surpassing the threshold ZT of 2 in a cost effective manner can enable significant usage of TE energy harvesting to convert waste heat in an automobile engine exhaust into electrical power [4]. Recently, Fairbanks noted that further improvements in ZT to approximately 10 could make TE power conversion competitive with the internal combustion engine [5]. Finally, Elder et al. stated that for automotive applications, TE utilization is possible if the module cost is brought down to approximately $0.10/W and a ZT-value above 3 can be achieved over a broad temperature range [6].

Relative to aircraft energy harvesting from power electronics, Hallinan et al. [7] showed that TE technology is already at a state where positive system level impact can be realized.

Transient behavior of the thermal-electrical energy conversion processes in TE devices for use in heat pumps has been a well studied topic [8-12]. As a cooler, the TE device instantly adsorbs electric energy at the p-n junctions when current is applied. Simultaneously, Joule heating results, but this thermal energy diffuses towards the p-n junction at a much slower rate than the electron flow. As a result, the TE device performance is temporarily enhanced until the Joule heating effects reach steady-state. When the TE device operates as a generator, Joule heating diffusion begins at the p-n junction when a temperature difference is applied across the device. Almost instantaneously, electrical energy adsorption commences, thus temporarily degrading the TE device performance until Joule heating reaches steady-state. For a typical bismuth telluride TE device, the transient effects occur for very small time durations on the order of 0.2 seconds, substantially lower than the time periods considered here.

The baseline waste heat recovery system without thermal switch source temperature modulation, shown schematically in Fig. 1 is proposed to harvest waste heat from a constant or variable heat source using TE devices. In this figure, illustrative source temperatures and power dissipation are plotted as a function of time. Also noted is the maximum allowable source temperature. In practice, this system must be designed for worst case heat input

scenarios due to variations in source heat output, sink temperature and thermal resistance, and manufacturing. This conservative design can force the system to operate well below the maximum temperature of the source, therefore reducing the temperature drop across the TE device and thus lowering the efficiency of the system. In order to compensate for these variations, the waste heat recovery system shown schematically in Fig. 2 is proposed to maximize the thermoelectric energy recovery from the system through the addition of a thermal switch, located between the source and the TE device. Again, in this figure, source temperature and power into the TE device are plotted as a function of time. The thermal switch ideally has controllable thermal resistance. As shown in the representative plot, when the heat input is near maximum, the thermal resistance of the thermal switch is set to a minimum to prevent the source from exceeding its maximum temperature. In this state the heat flows freely into the TE device, maximizing the temperature drop across the TE device and the efficiency of the energy harvesting system. When the heat input is off-peak, the thermal resistance is increased to dominate the thermal resistances in the system forcing energy storage in the heat source, thus causing an increase in a source temperature. In this state very little heat ideally flows through the TE device. Once the source temperature reaches the maximum operating temperature, the thermal resistance of the switch is once again minimized. This sequence of events repeats to allow greater work to be extracted from the system by restricting heat to flow through the TE device only during maximum source temperature and therefore maximum temperature drop across the TE device. This control results in greater time-averaged power output to power input ratios (PR).

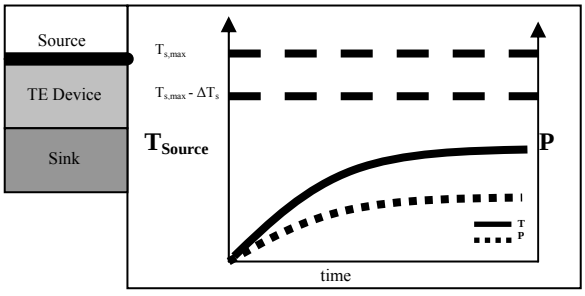

Fig. 1 Physical model of energy harvesting system without a thermal switch.

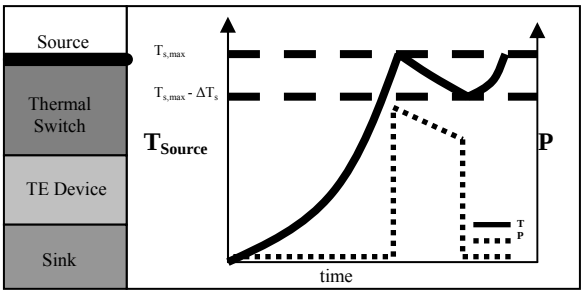

Fig. 2 Physical model of energy harvesting with a thermal switch.

In previous research, a finite difference analytical approach with source temperature feedback was used to evaluate the potential of source temperature modulation with a thermal switch on TE power output. The analytical model demonstrated that maximizing the exergy of the source, by maximizing its temperature during off-peak heat loadings, is capable of improving the time-averaged power output to power input ratio (*PR*) of a TE device. For some conditions, improved time-averaged power ratios of more than four times were realized. Criterion defining the operation space where power ratio improvements were developed. [13]

II. Experiment

To experimentally investigate the effects of a thermal switch on the waste heat recovery system, an experimental set-up comprised serially of a fixed heat source, a variable air gap serving as a thermal switch, a thermoelectric device and a heat sink mounted on a translation stage was employed. A schematic of this system is shown in Fig. 3. This set-up consists of a fixed heat source (silicon heater pad) attached to an aluminum or copper heat-spreader to simulate waste heat. This heat source assembly is mounted to a fixed plate located above a lower assembly that rests on a scissor jack driven by a stepper motor thereby permitting the lower assembly to be traversed up and down. Resting on top of the scissor jack, the TE device (Hi-Z HZ-2 Thermoelectric Module) is sandwiched between heat flux sensors and thermocouples. The heat sink, which is constructed of a copper plate with embedded tubing connected to a cooling bath pumping a 70/30 mixture of glycol to distilled water near -20°C, rests on top of the scissor jack. To represent the thermal switch in the high thermal resistance state, the stepper motor drives the scissor jack down until a desired air gap distance of 8 mm is achieved. Thus the high thermal resistance state is associated with conduction, radiation, and convection across the air gap. To represent the thermal switch in the low thermal resistance setting, the stepper motor drives the scissor jack up until the TE device is firmly pressed against the heat source assembly. When closed, the low thermal resistance between the heater assembly and the TE device is

dominated by the contact resistance between the TE device and heater spreader. Gentle pressure between heat source and TE device, achieved by application of a weight atop the "floating" heat source, ensures adequate thermal contact between the heater spreader and TE device.

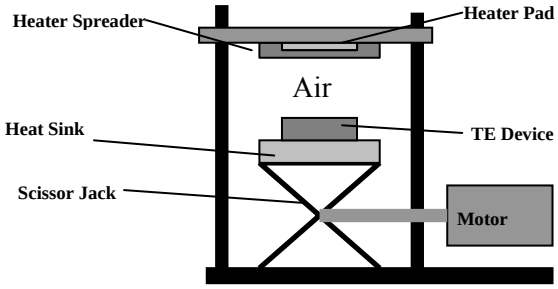

Fig. 3 Variable air-gap experiment set-up schematic.

The goal of this investigation is to determine the improvement of time averaged overall TE device power output to power input ratio (PR) for a waste heat recovery system with a thermal switch and compare it to a similar system without a thermal switch. The power ratio for the system (PR) is defined as the ratio of time averaged power generated by the TE device to the power into the system in the form of heat from the source as shown by equation (1).

$$PR = \frac{\dot{P}_{out}}{\dot{P}_{in}} = \frac{\int_0^T \dot{W}_{out}(t)dt}{\int_0^T \dot{Q}_{in}(t)dt} \tag{1}$$

The power ratio improvement due to switching is given by equation (2).

$$\text{PR Improvement} = \frac{PR_{switching} - PR_{no\_control}}{PR_{no\_control}} \tag{2}$$

Experiments were conducted for both constant heat and variable heat input. For the constant heat input tests, once the circulator (heat sink) reached a constant temperature, the heater pad (heat source, $\dot{Q}_{in}$) was set to a constant power setting to ensure that the source temperature with no thermal switching was 119 +/- 0.6 °C at the low thermal resistance setting. The air gap was set to zero guaranteeing firm contact between the heater assembly and the TE device. In this condition, the system achieved steady state (+/- 0.1 °C) prior to recording data to establish the system performance for no switching. Once this baseline was established, switching was employed by opening the air gap to a distance of 8 mm and monitoring the source temperature. Once the source temperature reached 158.5 +/-0.6°C,

the gap was once again zeroed. When the source temperature reached the lower bound, defined as $T_{s,\max} - \Delta T_s$, the air gap was again set to 8 mm and the process was repeated. The output power from the TE device was sampled every one second and the overall power ratio, PR, was calculated.

The variable heat input test began by determining the baseline, no control data set for a heat input described by equation (3).

$$\dot{Q}_{in} = \frac{\dot{Q}_{\max}}{2}\left(1 + \sin(\frac{f}{2\pi}t)\right) \tag{3}$$

where $\dot{Q}_{\max}$ was always set to 44 W and the frequency, f, was varied for each test. After the baseline was established, switching was employed as described above in the constant heat input test procedures.

III. Experimental Results

A. Constant Heat Input

For the constant heat input test, the ratio between the maximum source temperature for switching and the steady-state source temperature (no switching) was maintained at 1.333 by adjusting the heat input to the system. This ratio was set to mirror a safety factor built into design of a thermal management system.

The thermal resistances, capacitances, temperatures and thermoelectric properties were kept constant throughout the constant heat source test as summarized in Table 1.

Three source thermal capacitances were tested to determine the effects of source thermal capacitance on power ratio improvements. For each source capacitance tested, several different source temperature ranges, $T_{max} < T_s < T_s - \Delta T_s$, were considered in an effort to find the ΔT_s for each particular source capacitance which resulted in the greatest output power ratio for energy harvested.

Table 1 Physical and spatial variables that remain fixed for all constant heat input experimental cases studied.

Variable	Value
C_{TE}	25 J/^{o}K
R_{TE}	2.5 ^{o}K/W
$T_{s,steady}$	119 +/- 0.6 ^{o}C
$T_{s,\max}$	158.5 +/- 0.6 ^{o}C
T_{SINK}	-18.5 +/- 1.0 ^{o}C

$R_{P,LOW}$	1.75 ^{o}K/W
$R_{P,HIGH}$	120 ^{o}K/W
C_{SINK}	~∞ J/^{o}K
R_{SINK}	~0 ^{o}K/W
ZT_{eff}	0.1

As seen in Table 1, the effective ZT of the TE device was determined experimentally and is significantly lower than the company's published value of 1 [14], most likely due to the mounting procedures used in this test.

Figure 4 shows a plot of output power ratio improvement as a function of source temperature for the three source capacitances tested. As can be seen from the figure, an optimal ΔT_s exists for each source capacitance considered. If the ΔT_s value is too small, the time that the source is in contact with the TE device (energy is being harvested), t_{on}, is small in comparison to the time the source is not in contact with the TE device (no energy harvested), t_{off}, as seen in Fig. 5. If ΔT_s is too large, the source temperature drops to the point of degrading the output power of the TE device, as is observable in Fig. 6.

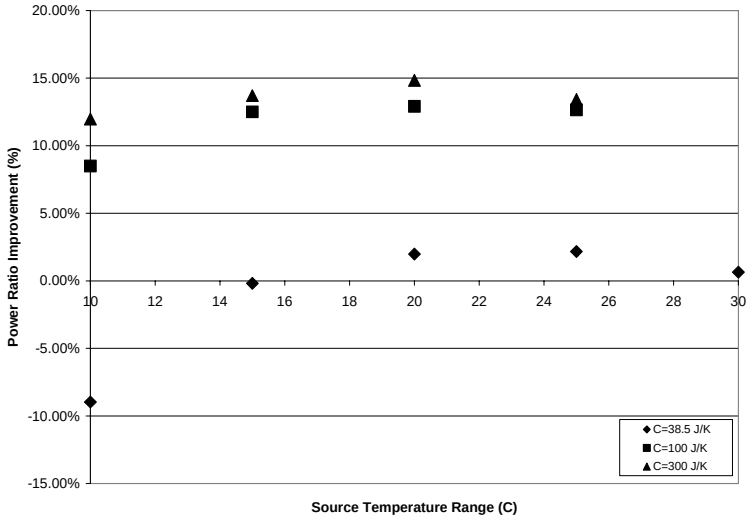

Fig. 4 Power output ratio improvements for constant heat input and C = 38.5, 100, and 300 $J/^{\circ}K$ as a function of ΔT_s.

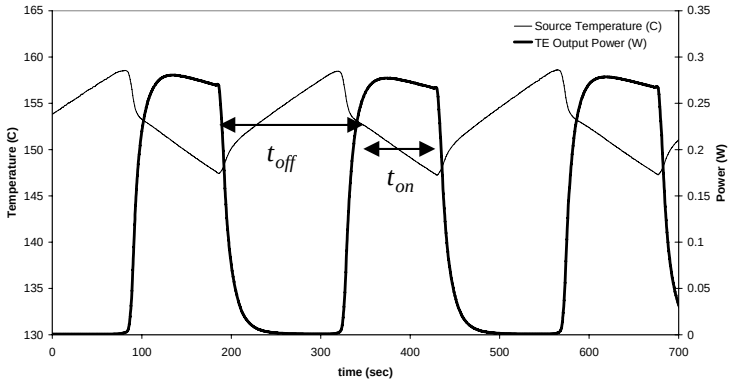

Fig. 5 Source temperature and TE output power for Case 2 with ΔT_s = 10°C.

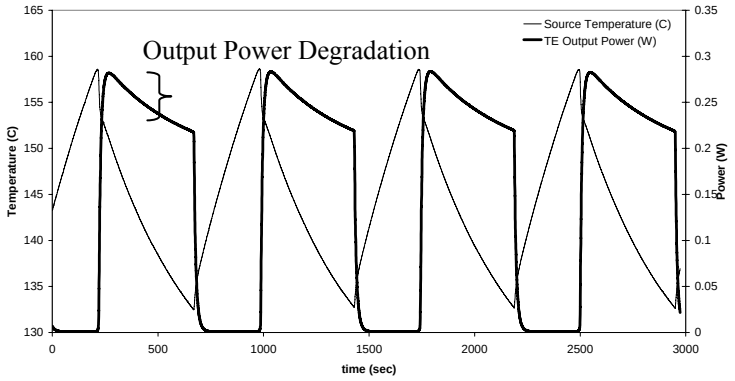

Fig. 6 Source temperature and TE output power for Case 2 with ΔT_s = 25°C.

Table 2 shows the optimal ΔT_s for each source capacitance tested. As the source thermal capacitance increases relative to the TE device thermal capacitance, the output power ratio improvement increases. Larger source capacitances allow the source to store more thermal energy when the thermal switch resistance is high. When the thermal switch resistance is low, more thermal energy can be forced through the system. When the thermal capacitance of the TE device is small in comparison to the source, relatively little energy is stored in the TE device, and thus the heat dissipated from the TE device when the thermal switch is off (at lower average temperature differences) is relatively small. The ratio of source contact time with the TE device, t_{on}, divided by time the source is not in contact with the TE device, t_{off} at optimal ΔT_s conditions is given as t_{on}/t_{off}. In all cases, for the experiments conducted the optimal on time versus off time ratio is about 1. This result is not a general rule, but a function of the experimental conditions. Experimental uncertainty of time-averaged power ratio improvement for the system was determined to be $\pm$ 0.17% and is reflected in the PR improvement measurements.

Table 2 Summary of the optimal experimental power output ratio improvements for constant heat input and variable source capacitance.

Case	$\dot{Q}_{in}$ (W)	C_S J/°K	$\Delta T_{s,opt}$ (°C)	t_{on}/t_{off}	Max PR Improvement (%)
1	27	38.5	25	1.01	2.17 ±0.17%
2	27	100	20	1.07	12.91 ±0.17%
3	32.7	300	20	1.01	14.84 ±0.17%

B. Variable Heat Input

For the variable heat input tests, the heat source capacitance was constant for all cases but the sinusoidal heat source input frequency was varied. Table 3 shows the fixed thermal resistances, capacitances, temperatures and thermoelectric properties for these tests. The frequency was changed from 0.003 Hz to 0.0003 Hz in order to better understand the effects of heat input frequency on PR .

Table 3 Physical and spatial variables that remain fixed for all variable input experimental cases studied.

Variable	Value
$\dot{Q}_{\max}$	44 W
C_S	100 J/°K
C_{TE}	25 J/°K
R_{TE}	2.5 °K/W
$T_{s,\max}$	160 +/- 0.6°C
T_{SINK}	-18.8 +/- 1.0 °C
$R_{P,LOW}$	1.75 °K/W
$R_{P,HIGH}$	120 °K/W
C_{SINK}	~∞ J/°K
R_{SINK}	~0 °K/W
ZT	0.1

To find the optimal output power ratio at each thermal load frequency, ΔT_s was varied until a maximum power improvement ratio was determined. As can be seen from Table 4, as the frequency decreases, the maximum source temperature without control, $T_{s,\max,nc}$, increases. Additionally, the output power ratio improvement was best in Case 2 for a frequency of 0.000556 Hz and ΔT_s =20°C. In Case 1, the high frequency heat input prevented the heat source from fully reaching its maximum value, therefore the power ratio improvement is degraded. In Case 3, the frequency is low enough that the non-negligible energy stored in the TE device is lost during open switch

conditions. This heat dissipation from the TE device during this period is associated with an effectively low temperature drop across the TE device, thus degrading the time-averaged power ratio improvement. One can conclude that the optimal frequency for energy harvesting for transient heat input would depend on the thermal capacitances of the source, TE device and the sink. If the thermal capacitance of the TE device is negligible, lower frequencies would produce more beneficial results with thermal switching.

Table 4 Summary of the experimental power output ratio improvements for variable heat input.

Case	f (Hz)	$T_{s,\max,nc}$ (C)	$\Delta T_{s,opt}$ (°C)	$\frac{t_{on}}{t_{off}}$	PR Improvement (%)
1	0.00333	102	20	0.472	20.00 ±0.17%
2	0.00056	130.6	20	0.517	30.04 ±0.17%
3	0.00028	150.8	30	0.630	25.82 ±0.17%

IV. Analysis

Building upon previous work of McCarty et al. [13], a finite difference thermal RC equivalent model of the TE energy recovery system, shown schematically in Fig. 7, was employed and can be compared experimental results.

A. Constant Heat

Using this finite difference model, the following thermal resistances, capacitances, temperatures and thermoelectric properties were kept constant throughout the constant heat source simulation, in an effort to represent the experimental set-up conditions, as shown in Table 5.

Table 5 Physical and spatial variables that remain fixed for all constant heat input simulated cases studied.

Variable	Value
C_{TE}	25 J/^{o}K
R_{TE}	2.5 ^{o}K/W
$T_{s,steady}$	118.8 ^{o}C
$T_{s,\max}$	160 ^{o}C
T_{SINK}	-20 ^{o}C
$R_{P,LOW}$	0.001 ^{o}K/W
$R_{P,HIGH}$	1,000 ^{o}K/W
C_{SINK}	100,000 J/^{o}K
R_{SINK}	0.0005 ^{o}K/W
ZT_{eff}	0.1

The finite difference model was used to predict the behavior of the waste heat recovery system with three different heat source thermal capacitances. $\dot{Q}_{in}$ was adjusted until the steady-state source temperature was 119 +/- 0.6°C. For each case studied, ΔT_s was varied until a maximum power ratio was determined analytically.

Table 6 shows the results for the analytical model with constant heat input. The $\dot{Q}_{in}$ necessary to achieve a steady-state source temperature of 119 °C was higher than compared to the experiment due to the differences in thermal resistances of the source and sink. The ratio of the source contact time, t_{on}/t_{off}, was slightly different for the analytical model due to the differences in experimental heat losses of the system. In both the analytical model and experiment results, the power ratio improvements increased as the thermal capacitance of the source increased. While the magnitude of the improvement was different, the trends were consistent.

Table 6 Summary of simulated power output ratio improvements for constant heat input.

Case	$\dot{Q}_{in}$ (W)	C_S J/°K	ΔT_s (°C)	$\frac{t_{on}}{t_{off}}$	Analytical PR Imp. (%)	Exp. PR Imp. (%)
1	55.5	38.5	30	1.14	2.41%	2.17 ±0.17%
2	55.5	100	25	1.5	8.03%	12.91 ±0.17%
3	55.5	300	20	2.5	21.63%	14.84 ±0.17%

V. Capacitance Effects

For the constant heat input experiments, it was noticed that as the source thermal capacitance increased at constant TE thermal capacitance, the output power ratio increased for both the experiment and finite difference simulation. To further investigate this phenomenon, the effect of different capacitance ratios, defined as the source thermal capacitance divided by the TE device thermal capacitance, on power output ratio was investigated. As can be seen from Fig. 8, increasing the capacitance ratio increases the output power ratio of the system with thermal switch control. Notably, when the thermal capacitance of the TE device is greater than the source, controlled thermal switching has no beneficial effect. For this case, heat transfer to the TE device causes significant thermal energy storage in the TE device. Thus, when the thermal resistance of the thermal switch is high, the thermal energy storage in the TE device is released at a smaller effective temperature drop across the device thus reducing overall

performance. Therefore the source thermal capacitance must be greater than the TE device thermal capacitance in order for thermal switching to be beneficial in waste heat recovery systems.

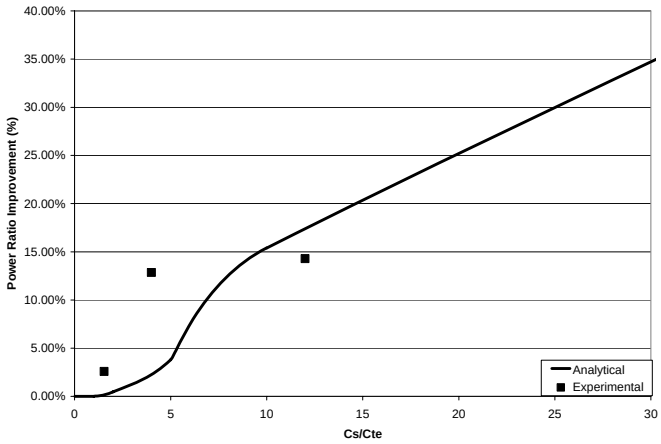

Fig. 7 Finite difference model and experimental power output ratio improvements as a function of thermal capacitance ratio.

VI. Comparison Between Model and Experimental Results

A plot of the source temperature and TE output power for the finite difference model with constant heat input is shown in Fig. 9a. A similar plot with the experimental data is shown in Fig. 9b. These plots for both the finite difference model and experiment for comparable input parameters are very similar. The finite difference model shows a maximum power ratio of 1.5%, with overall power improvement ratios increased by 21.6%. The maximum power ratio of the experimental system was 1.2%, with overall power improvement ratios increased by 14.8%. This discrepancy results from the finite difference model not accounting for the experimental heat loss to ambient. Also, the time required for the source temperature to reach its maximum allowable temperature for the analytical model is nearly 20% of the experiment because the of heat losses to the ambient during open state conditions in the experiments.

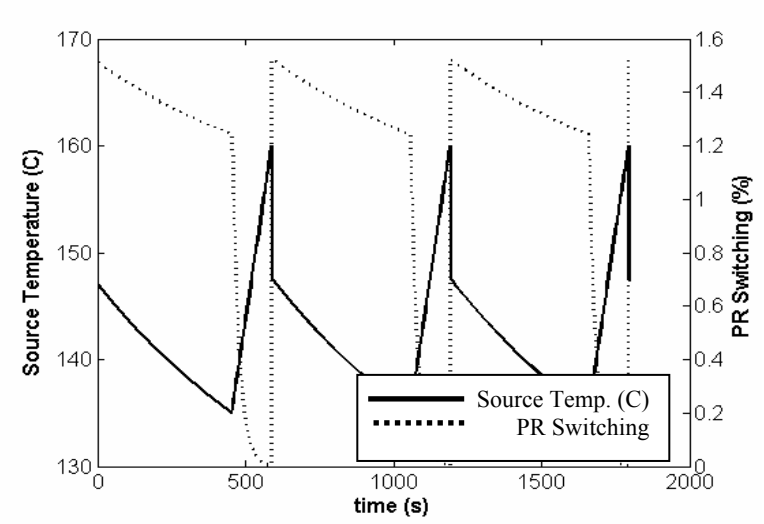

Fig. 8 Finite difference constant heat input for Case 3, $\dot{Q}_{in}$ =55.5 W, C_s =300 $J/^{\circ}K$, and $T_{s,\max}$ =160°C.

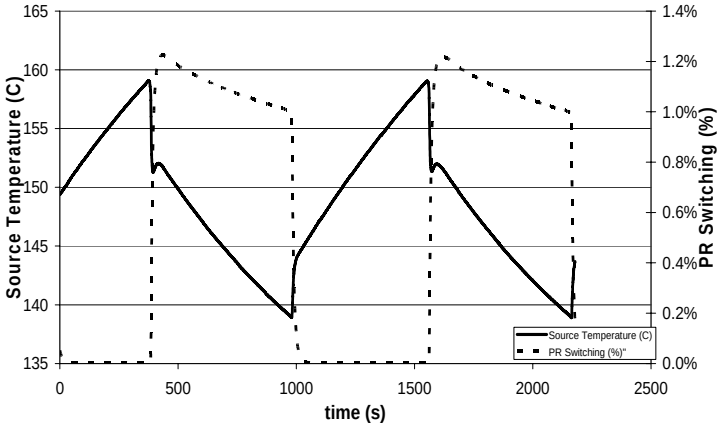

Fig. 9 Experimental constant heat input results for Case 3, $\dot{Q}_{in}$ =27 W, C_s =300 $J/^{\circ}K$, and $T_{s,\max}$ =160°C.

VII. Projected Results for State of the Art TE Device

While the *PR* improvements in the previous sections were notable, the overall efficiencies were still low because of the effective ZT of the TE used in the experiment. In order to better understand the effects of thermal switching for waste heat recovery systems with state-of-the-art TE devices, results for a state of the art TE device can be projected using the experimentally verified analytical model. For a waste heat recovery system operating at a maximum source temperature of 160°C, a source capacitance of 100 J/°K, a TE capacitance of 1 J/°K, and a ZT of 3,

the overall power output ratio could improve by more than 35% with a thermal switch as predicted by the finite difference model.

VIII. Conclusion

Both constant and variable heat inputs were tested experimentally using the variable air gap set-up. For constant heat input, several different heat source capacitances were considered. The sensitivity of changes in these parameters on the time-averaged efficiency was determined. For the variable heat input, several different heat input frequencies were also evaluated. Experimental power ratios for constant heat input improved up to 15% and for variable heat input improved up to 30% in certain design space conditions.

The experimental results provided in this paper prove that thermal switching can improve the performance of waste heat recovery systems that use TE devices. Also, the source thermal capacitance must be greater than the thermal capacitance of the TE device for thermal switching to improve output power recovered from a waste heat recovery system. Additionally, the experimental results verified the effectiveness of the analytical finite difference model developed in previous work. Finally, the analytical model predicted that thermal switching could boast a state-of-the-art waste heat recovery system output power ratio by 35% for constant heat input in certain design space conditions.

Acknowledgments

We would like to thank the Dayton Area Graduate Studies Institute and AFOSR for their continued funding and support and Hi-Z for the donation of the TE devices.

References

[1]Dresselhaus, M. S.; Lin, Y. M.; Black, M. R.; Rabin, O., Dresselhaus, G., "New directions for low dimensional thermoelectricity," *Materials Research Society Symposium Proceedings*, 2003, pp. 419-430.

[2]Venkatasubramanian, R., Viivola, E., Calpitts, T., and O'Quinn, B., "Thin film thermoelectric devices with high room temperature figures of merit," *Nature*, Vol. 413, No. 6856, 11 Oct., 2001, pp. 597-602.

[3]Martin, P.M. and Olsen, L.C., "Recent Progress in Scale Up of Multilayer Thermoelectric Films," *DOE/EPRI High Efficiency Thermoelectrics Workshop*, San Diego, CA, 17-20 February, 2004.

[4]Bell, L., 2004, "Thermoelectric Technology Readiness for Large Scale Commercialization," *DOE/EPRI High Efficiency Thermoelectrics Workshop*, 2004, San Diego, CA, 17-20 February.

[5]Fairbanks, J., "Chair's Overview of High Efficiency Thermoelectrics and Potential," *DOE/EPRI High Efficiency Thermoelectrics Workshop*, San Diego, CA, 17-20 February, 2004.

[6]Elder, A., Bertram, M., and Liebl, J., "Visions of Possible Thermoelectrics for Vehicle Applications," DOE/EPRI High Efficiency Thermoelectrics Workshop, San Diego, CA, 17-20 February, 2004.

[7]Hallinan, Kevin P. and Sanders, Brian, "Entropy Generation Metric for Evaluating and Forecasting Aircraft Energy Management Systems," *International Journal of Exergy*, Vol. 2, No. 2, 2005, pp. 120-145.

[8]Hoyos, G.E., Rao, K.R., and Jerger, D., "Fast Transient Response of Novel Peltier Junction," *Energy Conversion*, Vol. 17, No. 1, 1977, pp. 45-54.

[9]Stilbans, L.S., and Fedorovich, N.A., "The Operation of Thermoelectric Elements in Non-stationary Conditions," *Sov. Phys. Tech. Phys*. Vol. 3, 1958, pp. 460-462.

[10]Landecker, K., and Findlay, A.W., "Study of the Fast Transient behavior of Peltier Junctions," *Solid-State Electronics*, Vol. 3, 1961, pp. 239-260.

[11]Idnurm, M., and Landecker, K., "Experiments with Peltier Junctions Pulsed with High Transient Currents," *Journal of Applied Physics*, Vol. 34, No. 6, 2004, pp. 1806-1810.

[12]Gray, Paul E. "Approximate Dynamics Response Calculations for Thermoelectric Peltier-Effect Devices," *Solid-State Electronics*, Vol. 6, 1963, pp. 339-348.

[13]McCarty, R., et al., Enhancing Thermoelectric Energy Recovery via Modulations of Source Temperature for Cyclical Heat Loadings, *ASME Journal of Heat Transfer* (to be published).

[14]Ghamaty, S., and Elsner, N. B., "Quantum Well Thermoelectric Devices", *Proceedings of ASME InterPack*, 17-22 July, 2005, San Francisco, CA.